Nuclear Recoil Measurement in CsI(Tl) Crystal for Cold Dark Matter Detection

M.Z. Wang[a], Q. Yue[b], J.R. Deng[c], W.P. Lai[d,e], H.B. Li[a,d], J. Li[b], Y. Liu[b], B.J. Qi[c], X.C. Ruan[c], C.H. Tang[a], H.Q. Tang[c], H.T. Wong[d,†], S.C. Wu[a], B. Xin[c], Z.Y. Zhou[c]

[a] Department of Physics, National Taiwan University, Taipei, Taiwan

[b] Institute of High Energy Physics, Beijing, China

[c] Department of Nuclear Physics, Institute of Atomic Energy, Beijing, China

[d] Institute of Physics, Academia Sinica, Taipei, Taiwan

[e] Department of Management Information Systems, Chung Kuo Institute of Technology, Taipei, Taiwan

The potential merits of CsI(Tl) scintillating crystals for Dark Matter experiments make it a subject of recent interest. The scattering signatures by neutrons on a CsI(Tl) detector were studied using a neutron beam generated by a 13 MV Tandem accelerator. The energy spectra of nuclear recoils from 7 keV to 132 keV were measured, and their quenching factors for scintillating light yield were derived. The data represents the first confirmation of the Optical Model predictions on neutron elastic scatterings with a direct measurement on the nuclear recoils of heavy nuclei.

PACS Codes: 25.40.Dn, 95.35.+d, 29.40.Mc.
Keywords: Neutron elastic scattering, Dark matter, Scintillation detectors.

1. Introduction

The detection of Dark Matter and the studies of their properties [1] are of fundamental importance in particle physics and cosmology. The Weakly Interacting Massive Particles (WIMPs) are good candidates for "Cold" Dark Matter, and their experimental searches have gathered a lot of interests in recent years. The most promising avenue is to detect the nuclear recoil signatures due to elastic scatterings of WIMPs on the target isotopes. The typical energy depositions are only of the order of 10 keV, imposing big experimental challenges in terms of the detection of weak signals as well as background control at low energy close to detection threshold. A wide spectrum of experimental techniques is being pursued [2].

The DAMA experiment observed an annual modulation of nuclear recoil events [3] with NaI(Tl) scintillating crystal detectors, which can be interpreted as positive evidence of WIMPs due to the difference of the relative velocities of the Earth from the Halo sea within the year. This, however, contradicts the limit from the CDMS experiment [4] based on cryogenic technique.

There are potential merits of using CsI(Tl) scintillating crystals [5] for WIMP search and other low-energy low-background experiments [6, 7]. An experiment towards 200 kg of CsI(Tl) crystal scintillators to study low energy neutrino interactions at the Kuo-Sheng power reactor is being pursued [7], while the adaptation of the crystal for Dark Matter searches are the focus of several on-going projects [8,9] and an approved experiment [10].

One of the key issues to realize a Dark Matter search experiment with CsI(Tl) crystal scintillator is the studies of the experimental signatures of nuclear recoils due to WIMP-nuclei elastic scatterings. Nuclear recoils produce large charge density (dE/dx). The scintillating light output is expected to be reduced ("quenched") while the

timing profile of the pulse is different relative to the same energy deposition by minimum ionizing particles [11].

These signatures are the same as the nuclear recoil events produced by elastic scattering of neutrons on nuclei. The quenching factors measurement is reported in this article. They extend and improve on the work from the other recent measurements on CsI(Tl) [8,9], as well as on other scintillating crystals such as NaI(Tl) and CaF_2(Eu) [12].

2. Experimental Setup and Procedures

The experiment was performed at HI-13 Tandem accelerator at the China Institute of Atomic Energy (CIAE) in Beijing. A pulsed deuteron beam at 5.6 MeV interacted with a deuterium gas target in a cell (1 cm in diameter and 3 cm in length) at a pressure of 6 bar. Neutrons at 8.0 MeV kinetic energy with an RMS spread of 0.2 MeV were produced at zero degree. The CsI(Tl) sample was located 2.02 meters away from the deuterium target. Neutrons at zero degree were selected by a 32 mm by 35 mm collimator of length 1.2 m. The collimator were surrounded by shielding materials like iron, paraffin, lead and polyethylene to reduce background. During this data taking, the repetition rate of the pulsed beam was set at 4 MHz with 1 ns width and the average beam current was at 1 μA.

The scattering target, which also functioned as a detector, was a CsI(Tl) crystal scintillator[1] with diameter 3 cm and length 3 cm wrapped with Teflon sheets, aluminum foil and black plastic tape. To minimize supporting structures, the detector was hung at the correct position by a piece of string. The readout was achieved by a 29 mm diameter photo-multiplier tube (PMT).[2] The PMT signals passed through an amplifier and shaper and were digitized by a 20 MHz, 8-bit, Flash Analog-to-Digital Converter (FADC) [13]. The γ-response of the CsI(Tl) detector was calibrated with an LED pulser operated at single photo-electron intensity, as well as by standard ^{109}Cd and ^{133}Ba γ-sources. The calibration is 4 photo-electrons per keV of electron-equivalence energy.

Neutron tag was provided by liquid scintillator[3] detectors 105 mm in diameter and 50 mm in length equipped with PMT[4] readout and placed at various distance (r) and scattering angle (θ) from the target. The liquid scintillator provides pulse shape discrimination (PSD) capabilities for n-γ separation by commercial electronics[5]. The neutron tag signal was used to define the "START" timing for the time of flight (TOF) system. The pulsed deuteron "pick-off" signal provided by the accelerator was delayed and used as "STOP" for the TOF. The timing was arranged such that the STOP signal would always arrive before the next neutron pulse, so as to eliminate confused and accidental triggers. The (r,θ) configurations were chosen to optimize the TOF resolution to differentiate neutron elastic scatterings off protons from those of heavier nuclei in the wrapping materials and the CsI target.

The FADC recorded data continuously in a circular buffer of 4k size. A START-STOP sequence from the TOF system initiated a trigger which stopped the FADC digitization after 25 μs. The pulse shape from the CsI(Tl) crystal was recorded for a pre-trigger and post-trigger periods of 5 μs and 25 μs, respectively. The typical data taking rate with such trigger conditions was 4 Hz.

Data taking at each scattering angle was complemented by a measurement of the TOF background spectrum with *empty* target which was made of the CsI(Tl) wrapping materials only. Displayed in Figure 1 is the TOF spectra at 50° with empty and complete target. Faster neutrons have earlier START pulses resulting in larger TOF values. The "slower"(P_p at 36 ns) and "faster"(P_N at 48 ns) peaks are due to neutron elastic scattering off protons and the heavier nuclei such as C, Al, Cs and I, respectively. The flat background is due to random coincidence. It can be seen that with the CsI(Tl) target in place, P_N for neutron scattering off heavier nuclei becomes enhanced. The normalized difference between the two TOF spectra are the recoil events from Cs

[1] Producer: Unique Crystal, Beijing
[2] CR110, Hamamatsu Photonics, China
[3] Co-261, ST-451
[4] Philips XP-2041
[5] CANBERRA 2160A

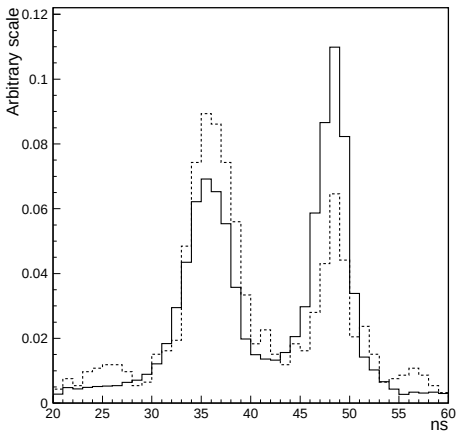

Figure 1. The TOF spectra at 50° scattering angle, for configurations with wrapping material only (dashed histogram) and with CsI(Tl) target (solid histogram).

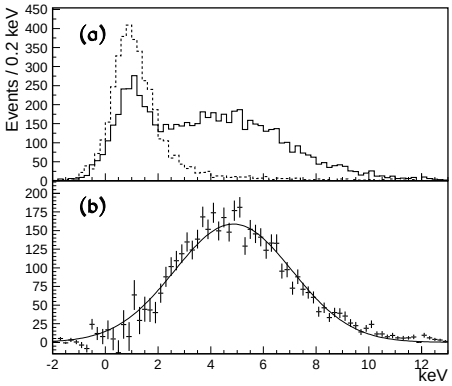

Figure 2. The CsI(Tl) recoil energy spectra at 50° scattering angle for (a) events at P_N (solid histogram) and P_p (dashed histogram), and (b) the subtracted excess fitted to a Gaussian.

and I.

The reconstructed energy of the CsI(Tl) target is defined as the pedestal-subtracted integrated area of the FADC pulse over 2.5 μs starting from the accurately-known "time-zero" of the CsI(Tl) events (which is 1.25 μs before the TOF trigger in this data taking). This restricted time window helps to minimize the pile up effect from accidental low energy γ's which are abundant along the beam line. Events are categorized into two groups by the central value between the two TOF peaks and their corresponding nuclear recoil energy spectra are compared.

Using the data set at 50° as illustrations, the energy spectra are displayed in Figure 2a for events under the P_N (solid histogram) and P_p (dashed histogram) peaks. The P_p events are triggered by proton recoils from the wrapping materials while having finite signals at the CsI(Tl) target due to accidental γ's. The spectrum shows a distinct peak with long tail on the high-energy side. This spectrum, scaled by a normalization factor f, should also contribute to the background in the P_N spectrum which originated from neutrons scattering off the heavier nuclei in the wrapping materials. The normalization factor f is the ratio of the P_p to P_N peaks in the empty target configuration in Figure 1. The detector response for CsI(Tl) nuclear recoil events can then be derived by subtracting f times the dashed histogram from the solid one in Figure 2a. Displayed in Figure 2b is the resulting spectrum with a Gaussian fit.

3. Measurement Results

The CsI recoil spectra obtained by the analysis scheme discussed in Section 2 were evaluated from the measurements of eight different scattering angles. The background levels away from the signal peaks after subtraction are always consistent with zero, showing the validity of this procedure. The mean light output and the number of observed events were derived from the centroid and area of Gaussian fits to the recoil spectra, respectively. The results are summarized in Table 1.

The nuclear recoil energy (T) is related to the neutron scattering angle (θ) by a simple kinematical formula:

$$\mathrm{T} = \frac{2\mathrm{A}}{(1+\mathrm{A})^2}\,(1-\cos\theta)\,\mathrm{E_n} \quad , \qquad (1)$$

where A is the target atomic mass and E_n is the incident neutron energy. The neutron scattering angle can be considered to be the same in this case in both the laboratory and center-of-mass

θ (°)	r (cm)	T (keV)	$E.E.$ (keV)	$Q.F.$ (%)
20	228	7.3	1.25 ± 0.20	17.1 ± 2.7
30	133	16.2	2.26 ± 0.27	14.0 ± 1.7
40	100	28.4	3.57 ± 0.57	12.6 ± 2.0
50	89	43.3	4.86 ± 0.49	11.2 ± 1.1
60	60	60.6	6.53 ± 0.65	10.8 ± 1.1
65	63	70.0	7.18 ± 0.72	10.3 ± 1.0
80	70	100	10.2 ± 1.0	10.2 ± 1.0
95	68	132	13.4 ± 1.3	10.1 ± 1.0

Table 1
Measured results on electron-equivalence light yield ($E.E.$) and quenching factor $Q.F.$ of the neutron elastic scatterings from the CsI(Tl) target, for different neutron scattering angle (θ) target-detector distance (r) and nuclear recoil energy (T). Errors shown are combined systematic and statistical uncertainties.

systems. Comparisons of the nuclear recoil spectra with those due to calibration sources allow the evaluation of the quenching factors, defined as the mean light yield from nuclear recoils versus that from γ sources.

As mentioned, a restricted integration time of 2.5 μs was adopted for the energy definition of the CsI(Tl) events, as compared to a typical complete light collection time of 12.5 μs. A correction factor of 1.15 is applied mean to the nuclear recoils light yield to account for this partial summation. This factor was derived by averaging and comparing a large number of events due to nuclear recoils and ^{109}Cd γ-source. The estimated uncertainty is 10%, based on studies with different integration time window from 1.5 μs to 12.5 μs.

The uncertainty of the mean nuclear recoil energy due to finite detector size is at most 2% for different scattering angles. This is checked by calculating this mean energy with proper weights of angular distributions, detector acceptance and the spread in neutron energy. A shift of detector at 1 mm scale has negligible effect on the central value of nuclear recoil energy. This uncertainty is small compared to that of the electron-equivalence light yield measurements shown in Table 1. The beam current was stable at the 1% level, as indicated by the stable data acquisition rates and measurements from beam monitor counters. The statistical and systematic uncertainties are then combined in quadrature to give the total uncertainties for each data point. The results were cross-checked with an alternative pulse shape analysis algorithms[14]. Instead of statistical subtraction, nuclear recoil events were selected based on their different pulse shapes compared to γ-background. The consistency levels among these two analysis procedures provide an estimate of additional systematic uncertainties which amounts to 16% at the lowest energy point at 20°.

The measured quenching factors are depicted in Figure 3a, while the variation of electron-equivalence light yield (the "visible" energy) versus recoil energies are shown in Figure 3b. Previous measurements [8,9] are overlaid for comparison. There is a clear trend of less quenching towards low energy points. This measurement achieved a lower threshold and with improved uncertainties. The quenching factors are of the similar range to those for NaI(Tl), which are typically 25% for Na and 8% for I from Ref. [15]. A linear relationship is observed for our data set between the electron-equivalence light yield and the nuclear recoil energy. Data from Ref. [8] shows more quenching and deviates from the linear regime at high energy. This linearity in the CsI(Tl) response is different from the highly non-linear characterisitcs due to threshold effects observed in liquid scintillator [16] at the same range of recoil energy.

To derive the differential cross sections from the observed number of events, the data taking time, the acceptance (proportional to r^{-2}) and the efficiency correction factors have to be evaluated. The efficiency factors are due to the TOF selection criteria and background subtraction scheme. It is close to 100% for the well-separated TOF peaks, but is only 42% at 20° where there are overlap between the TOF peaks. The contributions from inelastic scattering leading to the low excited levels for ^{133}Cs and ^{127}I are expected to be less than 0.1% relative to the elastic processes.

After all the correction factors are taken into account, the measured angular distribution for neutron elastic scatterings off Cs and I is dis-

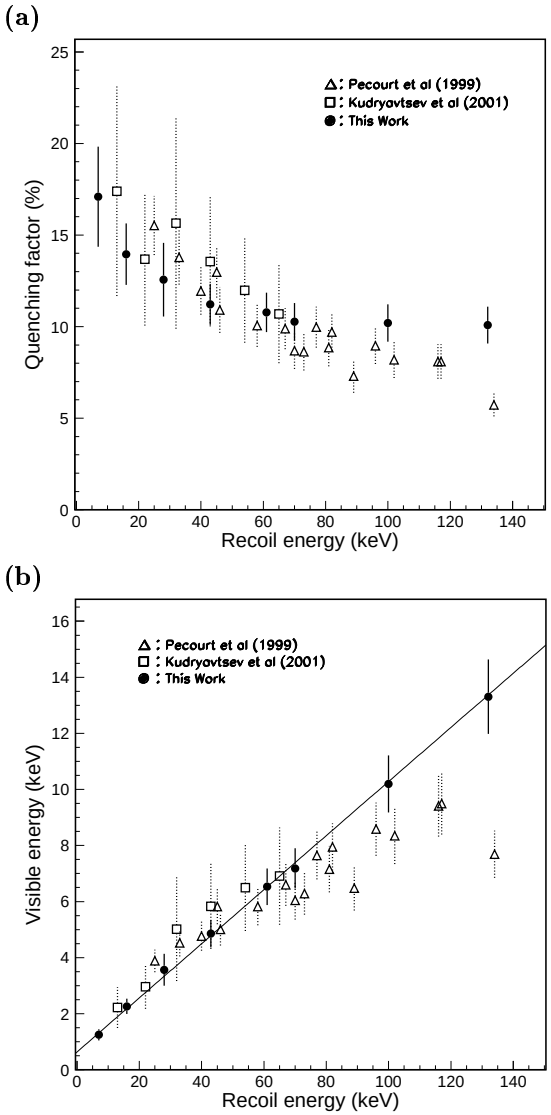

Figure 3. (a) The quenching factors and (b) electron-equivalence light yield versus recoil energy measured in this work (black circles), as well as in Ref. [8] (open triangles) and Ref. [9] (open squares).

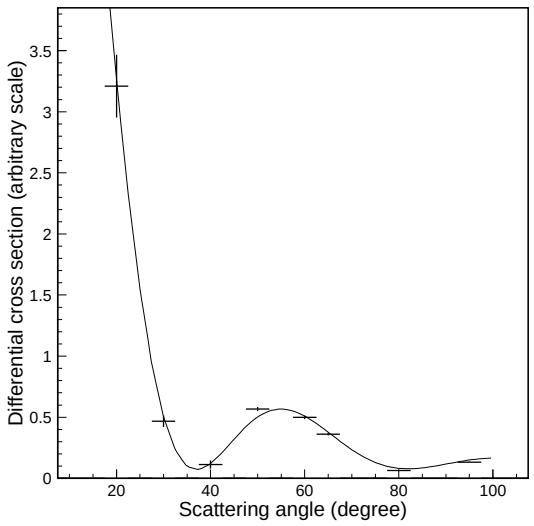

Figure 4. The measured nuclear recoil differential cross sections in CsI(Tl), superimposed with the Optical Model prediction.

played in Figure 4. The uncertainties are dominated by statistical errors from the subtraction procedures. The shape of the solid curve is due to the evaluated neutron elastic scattering cross sections on ^{133}Cs and ^{127}I from the ENDF/B-VI library [17] which originates from the Optical Model calculation. There is excellent agreement between the recoil angular distribution from this measurement and the predictions from the Optical Model. In particular, this is a kinematical regime where the size of the nuclei is comparable to the wavelength of the incident neutrons, and the diffraction pattern is well-reproduced by the data. The differential cross-section measurements demonstrate the validity of the analysis procedures at all angles, and provides an additional consistency check on the light yield results in Figure 3.

4. Discussion and Summary

In this article, we present a new measurement on the quenching factors of Cs and I in a CsI(Tl) crystal scintillator. Lower threshold and improved accuracies are achieved compared

to previous measurements. The measured differential cross-section of neutron scattering from I and Cs is in excellent agreement with Optical Model derivations, and represents the first confirmation of the Optical Model on neutron elastic scattering cross-sections with a direct measurement of nuclear recoils from heavy nuclei. That is, the neutrons do elastically scatter off from the nuclei but not via some anomalous processes. The recoil differential cross sections and the quenching factors are relevant to the studies of radiation damage in materials.

By optimizing the detector geometry and using green-extended photo-cathode, a detector with several kg modular mass and a light yield of a few photo-electron per keV can be realized [10]. The background considerations for CsI(Tl) detectors in terms of ambient radioactivity and intrinsic radio-purity are discussed in Refs. [6,7,18]. Levels of better than the 10^{-12} g/g level in concentration for the ^{238}U and ^{232}Th series have been demonstrated, assuming secular equilibrium. The potential problem of the internal ^{137}Cs contaminations can be overcome via selection of clean ore materials and careful chemical processing and purification treatment [10]. Given that the PSD capabilities for CsI(Tl) are better than those of NaI(Tl) and that there is matured experience of scaling up the CsI(Tl) detector to multi-ton systems, there are potentials of further improvements in the current sensitivities, and in the case of positive results, performing an accurate measurement of the annual modulation.

5. Acknowledgements

The authors would like to thank Drs. K.W. Ng, S.K. Kim and Y.D. Kim for fruitful discussions and helpful comments, and are grateful to the technical staff from CIAE and IHEP for operating the accelerator. This work was supported by contracts CosPa 89-N-FA01-1-4-2 from the Ministry of Education, Taiwan, NSC 89-2112-M-001-056 and NSC 90-2112-M-001-037 from the National Science Council, Taiwan, and NSF19975050 from the National Science Foundation, China. The support of H.B. Li is from contracts NSC 90-2112-M002-028 and MOE 89-N-FA01-1-0 under Prof. P.W.Y. Hwang.

† Corresponding author: htwong@phys.sinica.edu.tw

REFERENCES

1. For an overview, see, for example, E. Kolb and M. Turner, *The Early Universe*, Addison-Wesley (1989), and references therein.
2. For a recent review, see, for example, A. Morales, Nucl. Phys. B (Procs. Suppl.) **87**, 477 (2000), and references therein.
3. R. Bernabei *et al.*, Phys. Lett. **B 509**, 197 (2001), and references therein.
4. R. Abusaidi *et al.*, Phys. Rev. Lett. **84** 5699 (2000), and references therein.
5. H. Grassmann, E. Lorentz and H.G. Moser, Nucl. Instrum. Methods **228**, 323 (1985); P. Schotanus, R. Kamermans, and P. Dorenbos, IEEE Trans. Nucl. Sci. **37**, 177 (1990).
6. H.T. Wong *et al.*, Astropart. Phys. **14**, 141 (2000).
7. H.T. Wong and J. Li, Mod. Phys. Lett. **A 15**, 2011 (2000); H.B. Li *et al.*, TEXONO Coll., Nucl. Instrum. Methods **A 459**, 93 (2001); Y. Liu *et al.*, TEXONO Coll., Nucl. Instrum. Methods **A 482**, 12 (2002).
8. S. Pecourt *et al.*, Astropart. Phys. **11**, 457 (1999).
9. V.A. Kudryavtsev *et al.*, Nucl. Instrum. Methods **A 456**, 272 (2001).
10. H.J. Ahn *et al.*, Techical Design Report, KIMS Coll. (2001); H. Park *et al.*, nucl-ex/0202014, submitted to Nucl. Instrum. Methods **A** (2002).
11. See, for example, "Theory and Practice of Scintillation Counting", J.B. Birks, Pergamon (1964).
12. D.R. Tovey et al, Phys. Lett. **B 433**, 150 (1998).
13. W.P. Lai *et al.*, TEXONO Coll., Nucl. Instrum. Methods **A 465**, 550 (2001).
14. Q. Yue *et al.*, in preparation for Nucl. Instrum. Methods **A** (2002).
15. G. Gerbier *et al.*, Astropart. Phys. **11**, 287 (1999).
16. D.J. Ficenec *et al.*, Phys. Rev. **D 36**, 311 (1987).
17. http://www.nndc.bnl.gov, Evaluated Nuclear Data File (ENDF), National Nuclear Data Center, Brookhaven National Laboratory (2001).
18. U. Kilgus, R. Kotthaus, and E. Lange, Nucl. Instrum. Methods **A 297**, 425, (1990); R. Kotthaus, Nucl. Instrum. Methods **A 329**, 433 (1993).